On the Imaging of Hot Spots Using Correlation Radiometers and a Circular Aperture

GERD SCHALLER

Abstract—**A microwave correlation radiometer system with a circular synthetic aperture for the imaging of hot spots in homogeneous lossy tissue is investigated. Together with a proper reconstruction algorithm, the system has the ability to reconstruct correctly the position and the power density ratios of point-shaped noise sources. Results from computer simulations for various system parameters are presented in a graphical manner. Furthermore, it is shown that inexactly known attenuation and phase constants of the tissue vary the reconstructions only slightly.**

I. Introduction

THE NONINVASIVE measurement of the temperature of hidden objects is a challenging task not only in various fields of technology but also in medicine. For diagnosis and especially for the monitoring of hyperthermia treatments, technical systems with a good spatial and temperature resolution are needed. One possibility is to receive and measure the thermal noise power radiated from objects under investigation. According to Planck's law, the maximum of this electromagnetic radiation is in the infrared region for temperatures which are of interest in medicine; however, a small portion of this radiation is emitted in the microwave region, too. Generalizing, the lower the frequency, the lower the attenuation of tissue and therefore the better the possibility of measuring radiation at microwave frequencies from deeper parts of the body. Depending mainly on the water content, the penetration depth is a fraction of a millimeter in the infrared range, millimeters at millimeter waves, and up to several centimeters at lower microwave frequencies. Unfortunately, for a given aperture, spatial resolution is reduced in the same degree as the frequency. A way out of this dilemma seemed to be found when correlation techniques together with antennas with partially overlapping beams were introduced in [1]. The concept was to reduce the examined region to a small area common to both antenna diagrams. The same correlation principle, but with largely overlapping antenna patterns, a broad-band radiometer, and electronic scanning, was investigated in [2]. Likewise, largely overlapping antenna patterns are necessary in a system with a plane synthetic aperture for the scanning of large parts of the human body [3].

Manuscript received April 15, 1988; revised March 23, 1989.

The author is with the Institut fur Hochfrequenztechnik, Universitat Erlangen-Nurnberg, D-8520 Erlangen, West Germany.

IEEE Log Number 8928333.

A disadvantage of the systems proposed in the papers mentioned above is that they are lacking in a good radial resolution. To overcome this difficulty and to obtain the same spatial resolution in all directions, a circular aperture and a novel reconstruction algorithm were investigated both theoretically and experimentally in [4]. However, this small-band system suffered from relatively high side lobes in the reconstructed images. Considerable improvements have been achieved with a broad-band system of combined mechanical and electronic scanning [5]. Enhancing the bandwidth of a radiometer improves not only the imaging but also its sensitivity. It should be pointed out, however, that sensitivity problems are not analyzed here (see, for example, [2]). The purpose of this paper is to investigate the imaging properties of the proposed method by computer simulations. Additionally, the influence of important parameters on the reconstructions is discussed. The configuration is especially appropriate for the examination of smaller parts of the human body. For example, for the examination of the female breast the investigated system seems to be a useful approach.

II. System Considerations

The simplified model consists of an object space filled with a homogeneous and dissipative medium and one or more point-shaped noise sources within. To obtain a two-dimensional problem, it is presupposed that the noise sources lie in one plane, the object plane, and inside a circle. Despite the fact that the surrounding lossy matter emits radiation, too, we are only interested in the noise coming from the hot spots. The whole configuration must be stationary during a cycle of measurement. Measurements are performed using two omnidirectional antennas A_1 and A_2, positioned on a line through the center of the object plane and moved simultaneously to sample the signals at the circular aperture successively (Fig. 1). Corresponding to the bandwidth and the filter characteristic of the radiometer, a coherence area of hyperbolic shape, the position of which depends on the time delay adjustment, is formed in the object plane. By varying the time delay we can shift the coherence area, from which the system is able to detect signals, all over the object plane. In our case, the time delay is adjusted discontinuously in equal steps up to

0018-9480/89/0800-1210$01.00

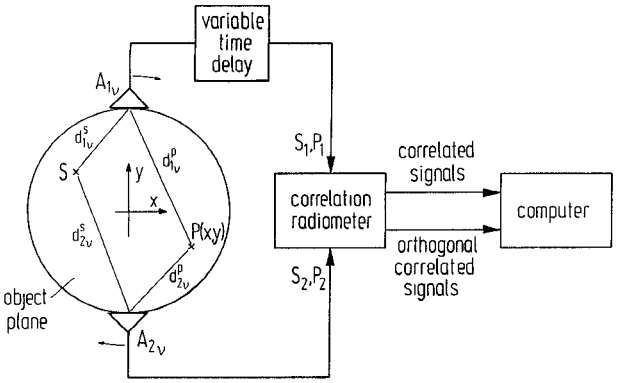

Fig. 1. Imaging system and relevant quantities.

a total number of M adjustments. As illustrated in [5], no imaging is possible utilizing measurements only at one antenna position, so for a total number of N antenna positions, we twist both antennas step by step for an angle of $180°/N$. At each antenna position an electronic scan must be performed by means of the time delay, realizable in the form of a line stretcher. If the measurement time in an experiment should be too long because of the successive sampling of the aperture, it is of course possible to employ more radiometer systems in parallel, up to a maximum number N. One possibility for realizing such a radiometer, delivering at its output both the correlated and the orthogonal correlated signals, was given in [4]. Obviously, the system described there can be modified in such a way that simultaneous measurements of both signals are possible. In any case, the computer has to store and process a set of $2MN$ "measured" values.

III. Theoretical Background

We consider one noise source S in the object plane, radiating the time-dependent signal $n(t)$, as is indicated in Fig. 1. Within the frequency range of interest, the source emits white noise of power spectral density N_s. The distances from S to the antennas A_1, A_2 are $d^s_{1_\nu}$, $d^s_{2_\nu}$ for the νth antenna position. To cross the distance d the signal is delayed by τ, where

$$\tau = d \cdot \frac{\sqrt{\epsilon_r}}{c_0} = d \cdot \frac{\beta}{\omega}. \tag{1}$$

Hence, at the input ports of the radiometer, the following signals can be obtained:

$$\begin{aligned} S_1(t) &\sim c_1^s \cdot n\left(t - \tau_1^s - \tau_l\right) \\ S_2(t) &\sim c_2^s \cdot n\left(t - \tau_2^s\right) \end{aligned} \tag{2}$$

with τ_l the time delay of the line stretcher and c_1^s and c_2^s the amplitude factors.

At the output of the radiometer we get the correlated signal S^c, and with the aid of a $\pi/2$ phase shifter, the orthogonal correlated signal S^o, according to

$$S^c \sim \lim_{T\to\infty} \frac{1}{2T} \int_{-T}^{+T} S_1(t) \cdot S_2(t)\, dt$$

and

$$S^o \sim \lim_{T\to\infty} \frac{1}{2T} \int_{-T}^{+T} S_1(t) \cdot S_2^o(t)\, dt \tag{3}$$

with $S_2^o(t) = S_2(t - T_0/4)$ and $T_0 = f_0^{-1}$, f_0 being the center frequency of the radiometer.

Equation (3) can be transformed to

$$S^c = G \cdot c_1^S \cdot c_2^S \cdot \phi_{nn}(\tau^s) \tag{4}$$

and

$$S^o = G \cdot c_1^s \cdot c_2^s \cdot \phi_{nn}^o(\tau^s)$$

where $\phi_{nn}(\tau^s)$ is the autocorrelation function of $n(t)$, $\phi_{nn}^o(\tau^s)$ is the orthogonal autocorrelation function, G is a factor including the overall gain, and $\tau^s = \tau_2^s - \tau_1^s - \tau_l$.

Applying theorems from system theory, we can further convert these relations, depending on the frequency response of the microwave test set. An ideal rectangular filter characteristic with a passband $f_0 \pm f_B$ yields

$$\begin{aligned} S^c &= 2G \cdot N_s \cdot c_1^s \cdot c_2^s \cdot \omega_B \cdot \mathrm{si}\left(\omega_B \tau^s\right) \cdot \cos\left(\omega_0 \tau^s\right) \\ S^o &= 2G \cdot N_s \cdot c_1^s \cdot c_2^s \cdot \omega_B \cdot \mathrm{si}\left(\omega_B \tau^s\right) \cdot \sin\left(\omega_0 \tau^s\right) \end{aligned} \tag{5}$$

with $\mathrm{si}(x) = \sin(x)/x$, whereas a Gaussian band-pass filter leads to

$$\begin{aligned} S^c &= \sqrt{2\pi} \cdot G \cdot N_s \cdot c_1^s \cdot c_2^s \cdot \omega_B \cdot \exp\left[-\frac{1}{2}(\tau^s)^2 \cdot \omega_B^2\right] \cdot \cos\left(\omega_0 \tau^s\right) \\ S^o &= \sqrt{2\pi} \cdot G \cdot N_s \cdot c_1^s \cdot c_2^s \cdot \omega_B \cdot \exp\left[-\frac{1}{2}(\tau^s)^2 \cdot \omega_B^2\right] \cdot \sin\left(\omega_0 \tau^s\right). \end{aligned} \tag{6}$$

Until now we have only assumed one noise source to be situated in the object plane. Now the question arises of the composition of signals S^c and S^o when there are several independent sources lying in the area of investigation. Taking the number of sources W, it follows from (2) that

$$\begin{aligned} S_1(t) &\sim \sum_{u=1}^{W} c_{1_u}^s \cdot n_u\left(t - \tau_{1_u}^s - \tau_l\right) \\ S_2(t) &\sim \sum_{v=1}^{W} c_{2_v}^s \cdot n_v\left(t - \tau_{2_v}^s\right) \end{aligned} \tag{7}$$

and from (3) that

$$S^c \sim \sum_{u=1}^{W} \sum_{v=1}^{W} \lim_{T\to\infty} \frac{1}{2T} \int_{-T}^{+T} c_{1_u}^s \cdot c_{2_v}^s \cdot n_u \cdot n_v\, dt. \tag{8}$$

Because of the fact that signals from different sources are not correlated, it follows that

$$\lim_{T\to\infty} \frac{1}{2T} \int_{-T}^{+T} c_{1_u}^s \cdot c_{2_v}^s \cdot n_u \cdot n_v\, dt = 0 \qquad \text{for } u \neq v \tag{9}$$

and therefore we can conclude that

$$S^c = G \cdot \sum_{u=1}^{W} c_{1_u}^s \cdot c_{2_u}^s \cdot \phi_{n_u n_u}(\tau^s) \tag{10}$$

or

$$S^c = G \cdot \sum_{u=1}^{W} S_u^c \tag{11}$$

holds. In analogous fashion, the same relation is valid for

$$S^o = G \cdot \sum_{u=1}^{W} S_u^o \tag{12}$$

and so the total signals S^c and S^o are the sum of W individual signals. In an experiment, the quantities S^c and S^o are directly measured; in computer simulations we can use (5) or (6) to calculate them. In any event, S^c and S^o serve to form a new complex quantity; that is, for the νth antenna position and for the μth time delay $\tau_{l\mu}$ we define

$$S_{\nu\mu} = S_{\nu\mu}^c + jS_{\nu\mu}^o = |S_{\nu\mu}| \cdot \exp\left(j\omega_0 \tau_\mu^s\right). \tag{13}$$

For numerical simulations, and, as will be seen later, for the reconstruction process, we need the amplitude factors c_1^s and c_2^s. Assuming isotropic radiation and knowing the attenuation constant α for the noise wave in the lossy matter leads to

$$c_{1,2} = e^{-\alpha \cdot d_{1,2}} \cdot \frac{A_{1,2}}{2 \cdot \sqrt{\pi} \cdot d_{1,2}} \tag{14}$$

provided the far-field approximation is justified. In this formula $A_{1,2}$ denote the effective areas of the two antennas.

Hence, with the abbreviation

$$C = \frac{\sqrt{A_1 \cdot A_2} \cdot G \cdot \omega_B}{2\sqrt{2\pi}}$$

for a given system, (13) together with (6) can be written as

$$S_{\nu\mu} = C \cdot N_s \cdot \frac{1}{d_{1_\nu}^s \cdot d_{2_\nu}^s} \cdot \exp\left[-\alpha \cdot \left(d_{1_\nu}^s + d_{2_\nu}^s\right)\right] \cdot \exp\left[-\frac{1}{2}\left(\tau_{2_\nu}^s - \tau_{1_\nu}^s - \tau_{l\mu}\right)^2 \cdot \omega_B^2\right] \cdot \exp\left[j\omega_0 \tau_\mu^s\right]. \tag{15}$$

As already mentioned, the time delay is adjusted discontinuously. For a total number of M adjustments we formally choose the time delay of the μth step as

$$\tau_{l\mu} = \frac{\mu}{M} \cdot 4R_0 \cdot \frac{\sqrt{\epsilon_r}}{c_0} \tag{16}$$

with μ an integer between $-(M-1)/2$ and $(M-1)/2$, M an odd number, and R_0 the radius of the object plane, which can be scanned nearly totally in this way.

In the reconstruction process we now need antenna signals produced only by a fictitious noise source P with the constant spectral power density N_p. This active probe is moved in small steps all over the object plane, and in each position x, y the radiometer signals can be computed for each antenna position analogous to (15). In contrast to the "measurement" procedure, where the time delay is varied in M steps, for the actual probe position τ_l is adjusted in an optimum manner. This means that the time delay difference of the signals to the two input ports of the radiometer must be minimum. For the probe $P(x, y)$ and the νth antenna position we therefore define

$$\tau_\nu^p = \min\left|\tau_{2_\nu}^p - \tau_{1_\nu}^p - \tau_l\right| \tag{17}$$

and denote the necessary adjustment to satisfy (17) $\tau_l = \tau_{l\nu}^p$.

Now, for the complex signal coming from the probe we obtain

$$P_\nu(x, y) = C \cdot N_p \cdot \frac{1}{d_{1_\nu}^p \cdot d_{2_\nu}^p} \cdot \exp\left[-\alpha \cdot \left(d_{1_\nu}^p + d_{2_\nu}^p\right)\right] \cdot \exp\left[-\frac{1}{2}\left(\tau_\nu^p\right)^2 \cdot \omega_B^2\right] \cdot \exp\left[j\omega_0 \tau_\nu^p\right]. \tag{18}$$

For calculating the ambiguity function at the position x, y from the measured values we use only the one we gained for the same optimum time delay adjustment $\tau_{l\nu}^p$. So from (15) it follows that

$$S_\nu^p = C \cdot N_s \cdot \frac{1}{d_{1_\nu}^s \cdot d_{2_\nu}^s} \cdot \exp\left[-\alpha \cdot \left(d_{1_\nu}^s + d_{2_\nu}^s\right)\right] \cdot \exp\left[-\frac{1}{2} \cdot \left(\tau_{2_\nu}^s - \tau_{1_\nu}^s - \tau_{l\nu}^p\right)^2 \cdot \omega_B^2\right] \cdot \exp\left[j\omega_0\left(\tau_{2_\nu}^s - \tau_{1_\nu}^s - \tau_{l\nu}^p\right)\right]. \tag{19}$$

We can now define the ambiguity function

$$\chi(x, y) = \mathrm{Re}\left\{K \sum_{\nu=1}^{N} \frac{S_\nu^p}{P_\nu(x, y)}\right\} \tag{20}$$

with K a normalizing factor, so that $\max[\chi(x, y)] = 1$. Taking the real part of the function (20) and twisting the antennas half a circle is equivalent to twisting the antennas a full circle and taking the complex sum, a fact which is not proved here.

The inverse formulation of the ambiguity function (20) is one possibility among others; a second convenient algorithm may be the "matched filter" approach according to

$$\chi(x, y) = \mathrm{Re}\left\{K \sum_{\nu=1}^{N} S_\nu^p \cdot P_\nu^*(x, y)\right\}. \tag{21}$$

As we will see later, reconstructions according to the two algorithms differ slightly.

In the images given below, negative values of the ambiguity function are set zero; thus

$$B(x, y) = \begin{cases} \chi(x, y) & \text{for } \chi > 0 \\ 0 & \text{otherwise} \end{cases} \tag{22}$$

is presented graphically.

To exemplify the relations above we finally assume the fictitious probe positioned exactly at the position x_0, y_0 of a noise source in the object plane. Furthermore, τ_l will be adjustable in arbitrary small steps. In this case we obtain for all antenna positions

$$d_{1_\nu}^p = d_{1_\nu}^s \qquad d_{2_\nu}^p = d_{2_\nu}^s \qquad \tau_\nu^p = 0$$

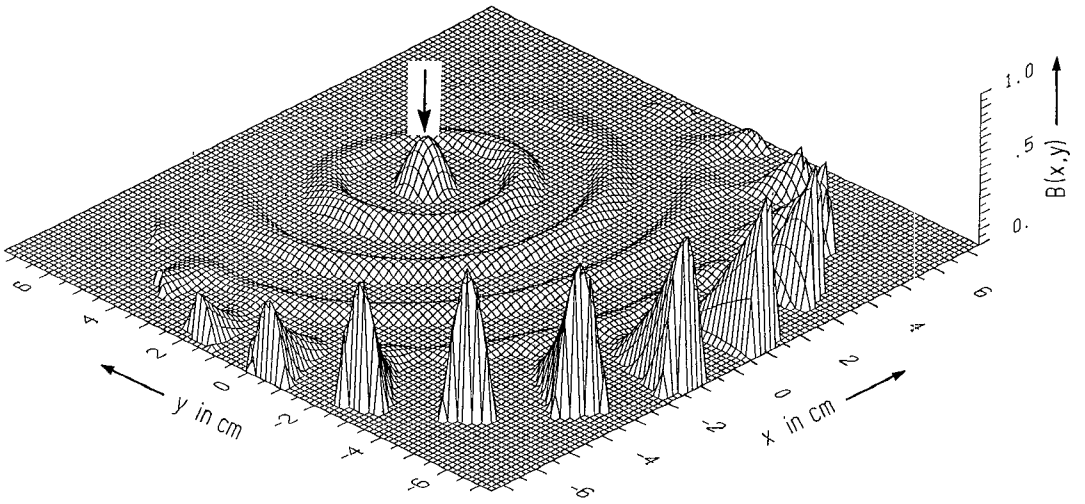

Fig. 2. Reconstruction of a noise source with only a few aperture samples ($N=14$; $M=1$).

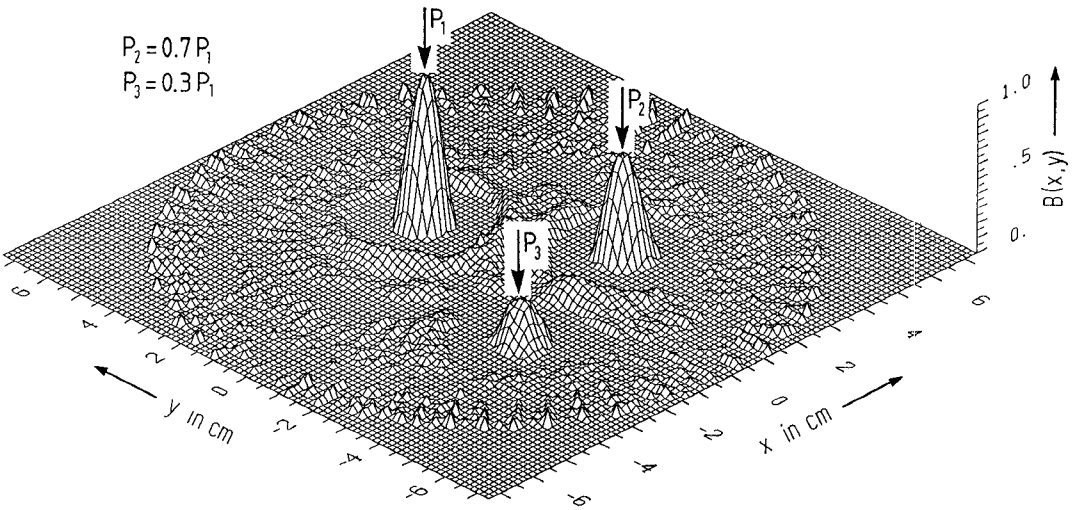

Fig. 3. Reconstruction of three noise sources according to eq. (20).

and

$$\tau_{l_\nu}^{p} = \tau_{2_\nu}^{p} - \tau_{1_\nu}^{p} = \tau_{2_\nu}^{s} - \tau_{1_\nu}^{s}$$

and so (20) results in

$$\chi(x_0, y_0) = N \cdot K \cdot \frac{N_s}{N_p} \tag{23}$$

a value proportional to the spectral power density of the source to be imaged.

IV. Simulated Results

For the diameter of the synthetic aperture we choose 15 cm. The hot spots are embedded in a medium with an attenuation constant $\alpha = 0.29$ cm^{-1} and a phase constant $\beta = 1.8$ cm^{-1} at the central frequency $f_0 = 1$ GHz of the radiometer. Data from radiometers of different bandwidths and frequency responses are used for reconstructions. In all figures the true positions of the noise sources are indicated by arrows.

In order to minimize the "measuring" time for the total set of $2MN$ values, it is advantageous not to exceed the necessary number of antenna positions N, or the number of time delay adjustments M substantially. On the other hand, a certain number of antenna positions are necessary to banish ambiguities out of the imaging region. This is illustrated in Fig. 2 for a small-band system with a too small number N and with ambiguities appearing partly at the rim of the image plane. The optimum number M depends on the bandwidth of the radiometer. The coherence area should be shifted in such a way that we are potentially able to receive signals from any source with nearly maximum amplitude.

The reconstructions of three noise sources with different power densities are performed in Figs. 3 and 4. Both figures are based on a broad-band radiometer with $f_0/f_B = 3$, $N = 30$, and $M = 31$ and with an ideal filter characteristic according to (5). Whereas Fig. 3 is calculated using the algorithm given in (20), Fig. 4 shows the reconstruction of the same configuration evaluating the ambiguity function after (21).

In all examples up to now we have investigated the imaging assuming a precise knowledge of the material

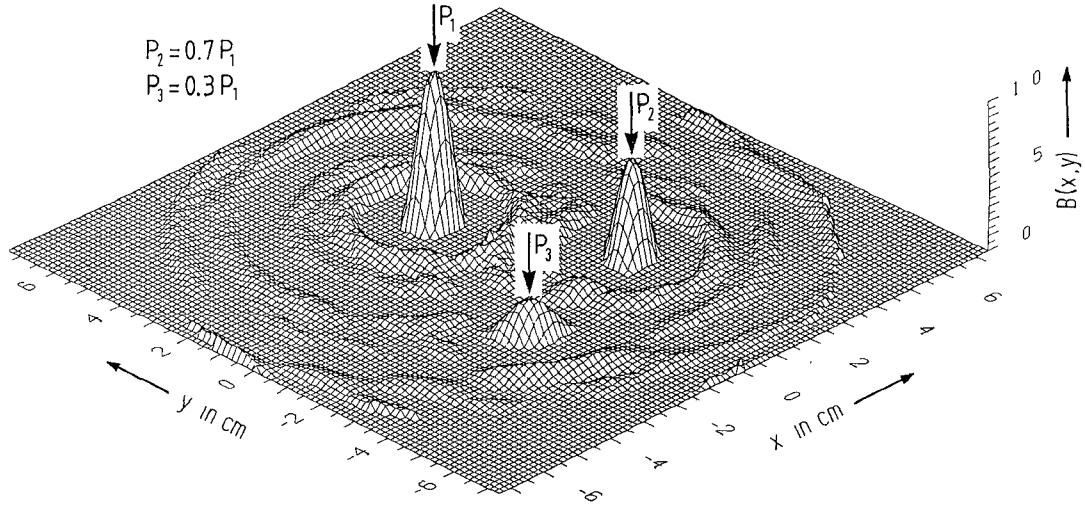

Fig. 4. Reconstruction of three noise sources according to eq (21).

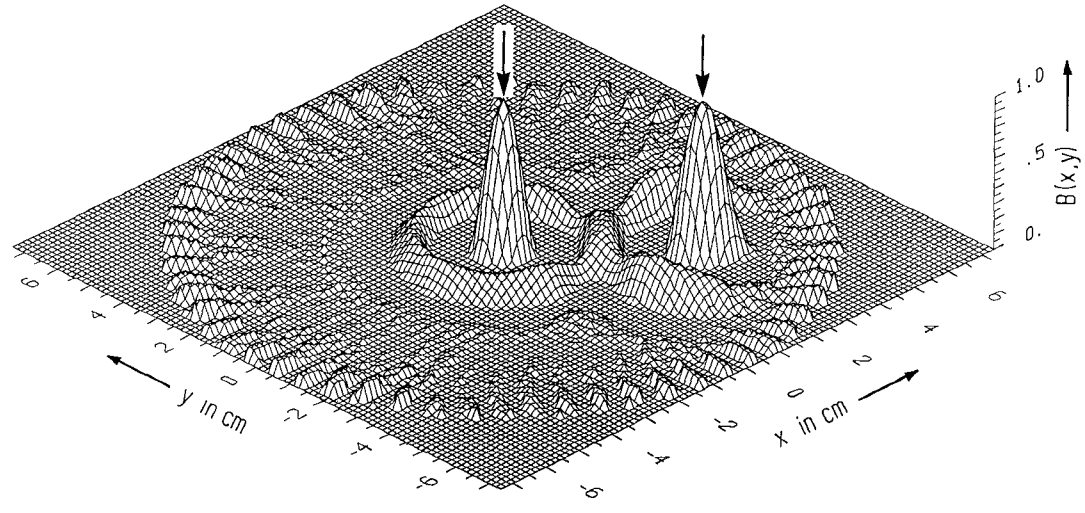

Fig. 5. Reconstruction of two noise sources: $\alpha^p = \alpha^s$; $\beta^p = \beta^s$.

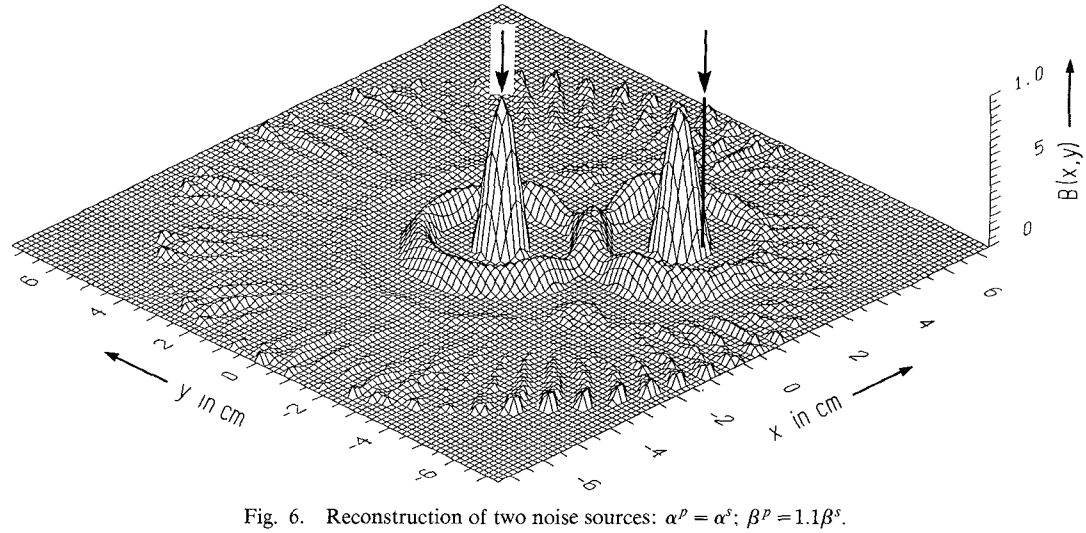

Fig. 6. Reconstruction of two noise sources: $\alpha^p = \alpha^s$; $\beta^p = 1.1\beta^s$.

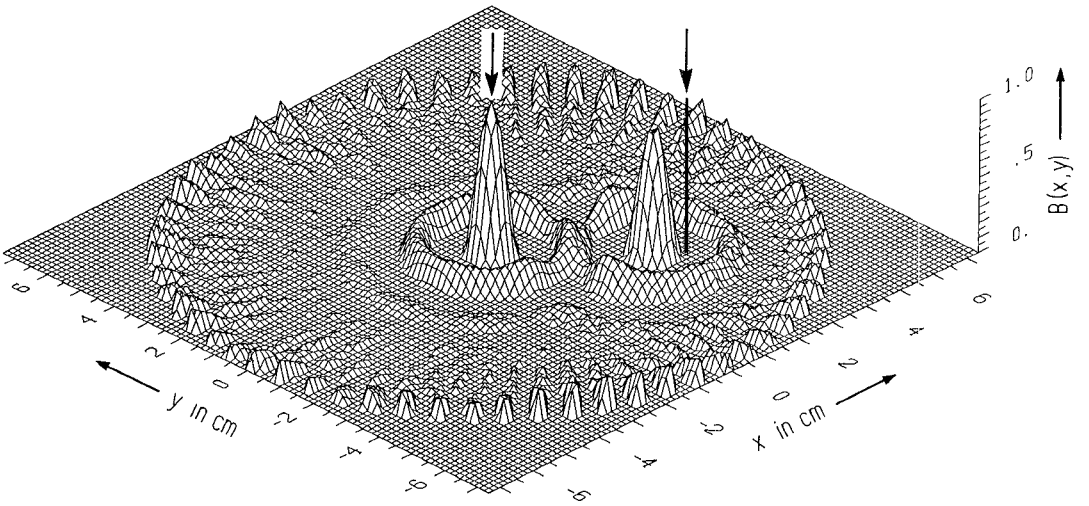

Fig. 7. Reconstruction of two noise sources: $\alpha^p = \alpha^s$; $\beta^p = 1\,2\beta^s$.

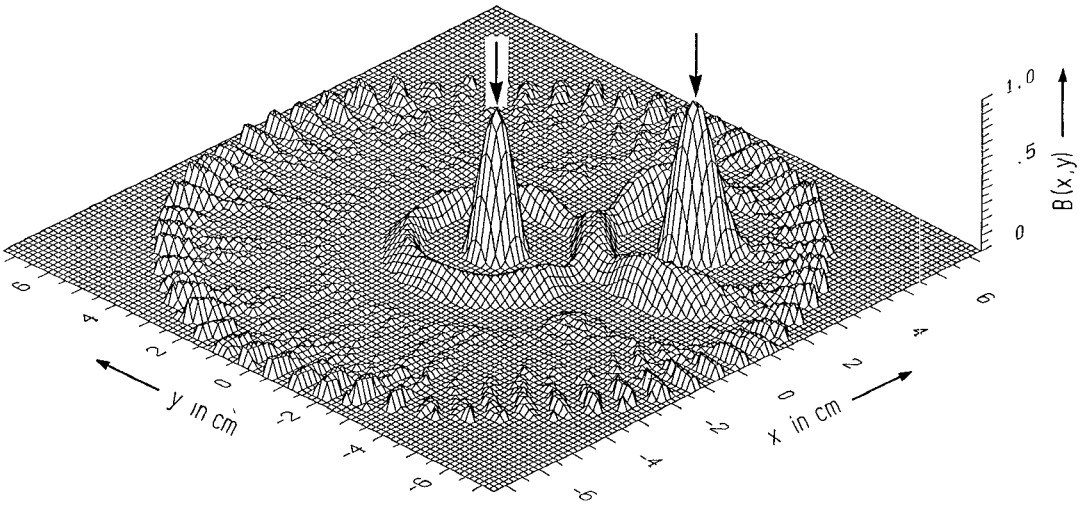

Fig. 8. Reconstruction of two noise sources: $\alpha^p = 1.2\alpha^s$; $\beta^p = \beta^s$.

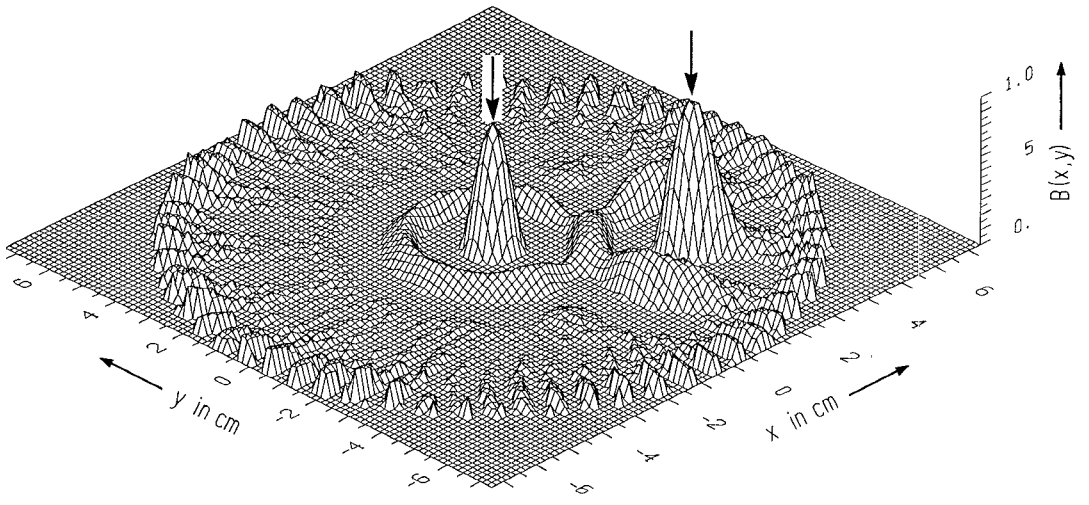

Fig. 9. Reconstruction of two noise sources: $\alpha^p = 1.5\alpha^s$; $\beta^p = \beta^s$.

parameters of the object space; i.e., in the reconstruction algorithm we used the same attenuation and phase constant for the probe signals as for the evaluation of the source signals. This assumption, however, idealizes matters to quite an extent and is not reflected in reality. So the problem arises of how the reconstructions vary if α and β are not known exactly. To answer this question we form $\alpha = \alpha^p$, $\beta = \beta^p$ in (18) and $\alpha = \alpha^s$, $\beta = \beta^s$ in (19). Figs. 5 to 9 illustrate the reconstructions of two noise sources of equal power for various ratios α^p/α^s and β^p/β^s. Calculations are based on a radiometer with a Gaussian frequency response, a bandwidth $f_0/f_B = 6$, $N = 30$ antenna positions, and $M = 19$ time delay adjustments. By comparison, the reconstruction according to (20) with $\alpha^p = \alpha^s$ and $\beta^p = \beta^s$ is given in Fig. 5. For the same configuration, the phase constant is falsified with a 10 percent deviation in Fig. 6. As can be seen, the amplitude ratios of the two sources are nearly unchanged; mainly the position of the source distant from the center is shifted nearer to the center. This effect is evident in an enhanced degree in Fig. 7, where a 20 percent deviation is assumed for the phase constant.

Summarizing, we can conclude that an uncertainty in the phase constant results in an uncertainty of the source distance to the center. Furthermore, this error is also proportional to the distance from the center. Depending on the sign of the error, sources are shifted to or off the center.

Finally, in Figs. 8 and 9 we can see how erroneous attenuation constants affect the reconstructions. As we can expect, the amplitude ratios are influenced by this error; however, the sensitivity for this error is relatively small. This is clearly demonstrated in Fig. 8 with a 20 percent difference in the attenuation constants, and also in Fig. 9, where even a 50 percent attenuation difference is assumed.

V. Conclusions

It has been shown that, with the simplifying assumptions of our model, a correlation radiometer in combination with a circular aperture is suited for the imaging of hot spots in lossy media. Even a faulty knowledge of the material parameters produces tolerable results. The investigated system has the decisive advantage that the spatial resolution is nearly constant in all directions and all over the object plane.

In future investigations the problem of thermal sensitivity and thermal resolution will be of interest, because correlation radiometers only indicate temperature gradients. However, owing to the thermal conductivity of the human body, these temperature gradients are not very steep.

Another essential restriction is the assumption of a homogeneous medium. It is evident that in the presence of a strong scatterer the simple relations given in Section III are no longer valid.

Acknowledgment

The author thanks A. Eitel for computations and interesting discussions. Part of the results have been obtained in cooperation with M. Schulz during his work at the institute.

References

[1] A. Mamouni, J. C. van de Velde, and Y. Leroy, "New correlation radiometer for microwave thermography," *Electron. Lett.*, vol. 17, no. 16, pp. 554–555, Aug. 6, 1981.

[2] J. C. Hill and R. B. Goldner, "The thermal and spatial resolution of a broad-band correlation radiometer with application to medical microwave thermography," *IEEE Trans. Microwave Theory Tech.*, vol. MTT-33, pp. 718–722, Aug. 1985.

[3] N. C. Haslam, A. R. Gillespie, and C. G. T. Haslam, "Aperture synthesis thermography—A new approach to passive microwave temperature measurements in the body," *IEEE Trans. Microwave Theory Tech.*, vol. MTT-32, pp. 829–835, Aug. 1984.

[4] G. Schaller, "Synthetic aperture radiometry for the imaging of hot spots in tissue," *Proc. 17th European Microwave Conf.* (Rome), 1987, pp. 902–907.

[5] G. Schaller, "Microwave correlation thermography for the imaging of hot spots in lossy materials," in *IEEE MTT-S Int. Microwave Symp. Dig.* (New York), 1988, pp. 155–156.

Gerd Schaller received the diploma in electrical engineering from the Technische Hochschule Munich, Munich, Germany, in 1965.

From 1966 to 1969 he worked at Grundig Electronic as a Research and Development Engineer on the design and development of electro-optic components and systems. In 1969 he joined the Institute for High Frequency Technology at the University Erlangen/Nuremberg, where he received the Dr.-Ing. degree in 1976. His research activities have been in the area of microstrip components; currently he is involved in microwave radiometry for medical purposes and in microwave hyperthermia.